esa

ECOSPHERE

EMERGING TECHNOLOGIES

Assessing the hydroregime of an archetypal riverine wet meadow in the central Great Plains using time-lapse imagery

EMMA M. BRINLEY BUCKLEY [1,†] ANDREW J. CAVEN [2] JOSHUA D. WIESE,[2] AND MARY J. HARNER [1,3]

[1]*Department of Communication, University of Nebraska at Kearney, Kearney, Nebraska 68849 USA*
[2]*Platte River Whooping Crane Maintenance Trust, Wood River, Nebraska 68883 USA*
[3]*Department of Biology, University of Nebraska at Kearney, Kearney, Nebraska 68849 USA*

Citation: Brinley Buckley, E. M., A. J. Caven, J. D. Wiese, and M. J. Harner. 2021. Assessing the hydroregime of an archetypal riverine wet meadow in the central Great Plains using time-lapse imagery. Ecosphere 12(11):e03829. 10.1002/ecs2.3829

Abstract. Wet meadows are a declining and increasingly degraded ecosystem type. They contribute numerous ecosystem services, including nutrient cycling, water storage, and filtration, and provision of wildlife habitat, particularly for wetland-dependent species such as the Whooping Crane (*Grus americana*). Conservation and restoration of wet meadows rely on understanding their hydrology but characterization of wet meadow hydroregimes is difficult given their hydrologic complexity, high variability, and distinct regional differences. To address this challenge, we used ground-based time-lapse imagery to assess inundation dynamics of an archetypal wet meadow over a six-year period in the Central Platte River Valley, Nebraska, USA. We analyzed over 6500 images from March 2011 to May 2017 in the open-source java-based image processing software ImageJ. We also obtained data on groundwater, streamflow, precipitation, and evapotranspiration. We assessed the relationship between wet meadow inundation and hydrologic variables using wavelet coherence to look at fluctuations across a time–frequency spectrum and used random forest to identify seasonally specific variables of importance. We found hydroperiod, the duration surface water ponded within the wet meadow, had a mean of 141 d, on average lasting from 10 December to 1 May, but varied annually. Inundation generally peaked in the early spring, on average 10 March, but demonstrated a bimodal distribution, peaking again in late spring during wetter years. While inundation responded rapidly to precipitation events, it was highly related to streamflow, while an elevated groundwater table was necessary for sustained inundation. Overall, our study provided a comprehensive hydrological characterization of a reference wet meadow and demonstrated the utility of time-lapse cameras for high-resolution monitoring and assessment of highly variable wetland systems. Considering the uncertainties surrounding land- and water-use changes, climate change, and the increasing demand for freshwater resources by growing human communities, understanding functional wet meadow hydroregimes and interrelated drivers is essential to inform wet meadow restoration, conservation, and management efforts.

Key words: hydrologic regime; hydrology; image analysis; inundation; Nebraska; Platte River; time lapse; wavelet; wet meadow; wetland.

Received 12 March 2020; revised 22 May 2021; accepted 24 June 2021. Corresponding Editor: Judy Cushing.

† **E-mail:** emmabrinleybuckley@gmail.com

Introduction

Hydrologic variability is a defining characteristic of wet meadows and essential to their maintenance and function (Tiner 2016). As palustrine wetlands structured by wet–dry cycles, wet meadows have dynamic hydroregimes and support a number of rare and threatened species (Nagel and Kolstad 1987, Whiles and Goldowitz 2005, Riggins et al. 2009, Vivian et al. 2013). In the Great Plains of North America, wet meadows generally exist along a hydrological gradient between terrestrial lowland prairies and shallow marshes, which are wetlands with longer duration hydroperiods (a continuous period of inundation; Kantrud et al. 1989, Kirby et al. 2002, Tiner 2016). Sustained inundation or a lack of periodic inundation can result in the ecosystem transitioning to a different stable state (Boswell and Olyphant 2007, Zweig and Kitchens 2009).

Once relatively widespread throughout the Great Plains, wet meadows have been extensively degraded or lost due to land and water-use changes (Laubhan and Fredrickson 1997, Rolfsmeier and Steinauer 2010). In the Central Platte River Valley (CPRV) of Nebraska, estimated wet meadow losses exceed 70% over the last century as a result of reduced river flows, groundwater withdrawals, and conversion to cropland and human development (Sidle et al. 1989). The limited remaining wet meadows face several continued threats including conversion to cropland and hydrological modification as well growing threats from tree and shrub invasion, invasive species, siltation and fertilization from adjacent cultivation, and climate change (Freeland et al. 1999, Dahl 2000, Galatowitsch et al. 2000, Gage and Cooper 2013, Wright and Wimberly 2013, Joyce et al. 2016). Restoration of wet meadows is challenging, and many restoration efforts are ultimately unsuccessful because of landscape-level alterations to the hydrogeomorphic processes that ultimately sustain them (e.g., increased groundwater depths; Boswell and Olyphant 2007, Riggins et al. 2009). Very few quality sites remain to serve as regionally specific references for restoration efforts, and even fewer have had their hydrological characteristics and dynamics thoroughly described. With continued pressure on freshwater systems globally (Vörösmarty et al. 2010), there is a need for high-resolution monitoring techniques to assess hydrologic change, particularly in vulnerable and increasingly degraded wetland systems.

Although wet meadow characteristics vary based on geographic location throughout the world, including montane, arid, and prairie landscapes, they share similar defining characteristics (Kantrud et al. 1989, Kindscher et al. 1997, Joyce et al. 2016). Wet meadows have hydric soil features, support wetland vascular plant species, and have temporary and recurrent hydroperiods (Keddy 2010, Gage and Cooper 2013, Tiner 2016). The intermittent cycles of inundation serve as a control over chemical and biological processes and disseminate biotic and abiotic material, creating heterogeneity and influencing species richness, abundance, production, and trophic structure (Currier 1989, Moorhead et al. 1998, Whiles and Goldowitz 2001, Gray et al. 2004, Henszey et al. 2004, Keddy 2010, Greenberg et al. 2015, Tiner 2016).

Wet meadows in the CPRV receive moisture from groundwater, streamflow, precipitation, and overland flooding, and the interplay among these drivers and how they vary seasonally are poorly understood (Hurr 1983, Wesche et al. 1994). Extensive time, money, and resources have been devoted to managing and restoring the Platte River's floodplain and associated habitats, as well as to understanding its interconnected hydrology (Hurr 1983, Wesche et al. 1994, Pfeiffer 1999, Henszey et al. 2004, Meyer et al. 2010). Albeit, due to the complex set of drivers, inherent periodicity, and high variability, wet meadow hydrology in the CPRV is challenging to study, and therefore, our understanding remains limited (Wesche et al. 1994, Riggins et al. 2009).

As wetland dynamics are often temporally heterogeneous, assessing change at higher frequency time intervals is important. In-person measurements and aerial and satellite imagery can be limited by financial resources and the temporal frequency of data collection. In-person measurements are often time-consuming, especially if data collection is conducted in remote areas, and by contrast, satellite imagery is often collected at a lower temporal frequency or image resolution than needed for monitoring highly variable ecological phenomena. Ground-based

cameras can overcome some of these challenges, filling a data-acquisition gap between satellite or aerial imagery and in-person field measurements (Morisette et al. 2009, Brinley Buckley et al. 2017). Increasingly, ground-based cameras have been used to monitor a range of ecosystem and hydrologic processes and dynamics (Parajka et al. 2012, Kramer and Wohl 2014, Gleason et al. 2015, Young et al. 2015, Keys et al. 2016, Brinley Buckley et al. 2017, Leduc et al. 2018). Our primary objective was to assess the hydroregime of an archetypal wet meadow in the CPRV using ground-based digital imagery over a six-year period and to determine the primary drivers of wet meadow inundation and seasonal variation therein. We predicted inundation would exhibit a strong seasonal signal associated with Platte River streamflow. Understanding the complex variability of these systems is necessary to establish a reference baseline, guide management, direct restoration, and consider implications for at-risk and endangered species in a changing landscape.

Methods

Study site

Mormon Island supports an archetypal wet meadow situated within the CPRV approximately 12 km southwest of Grand Island, Hall County, Nebraska, USA (Fig. 1; 40.799274, −98.416994). The 890-ha island is the largest contiguous parcel of lowland tallgrass prairie and wet meadow habitat remaining in the CPRV (Currier 1989). Historically, much of Mormon Island was too wet for agriculture and, thus, remained in a near-natural state as the surrounding landscape was converted to row-crop agriculture during the last century.

In the late 1970s, Mormon Island was protected for habitat conservation, notably for preservation of Whooping Crane (*Grus americana*) stopover habitat, as well as for the benefit of other migratory waterbirds (VanDerwalker 1982). Wet meadows in the CPRV provide critical stopover and/or breeding habitat in the Central Flyway for a diversity of migratory waterbirds and grassland birds, including the Sandhill Crane (*Antigone canadensis*), Marbled Godwit (*Limosa fedoa*), and Bobolink (*Dolichonyx oryzivorus*) (Lingle and Hay 1982, Skagen and Knopf 1993, Meine and Archibald 1996, Caven et al. 2019*c*). Wet meadow availability has likely limited the distribution of spring staging Sandhill Cranes in the CPRV (Faanes and LeValley 1993, Caven et al. 2019*a*) and is generally a preferred habitat for diurnal use by Whooping Cranes (Armbruster 1990, Baasch et al. 2019). In addition, CPRV wet meadows support a wide range of biodiversity, including anurans like the boreal chorus frogs (*Pseudacris maculata*; Geluso and Harner 2013, Brinley Buckley et al. 2021), regionally endemic macroinvertebrates such as the Platte River caddisfly (*Ironoquia plattensis*; Whiles et al. 1999, Geluso et al. 2011, Vivian et al. 2013), and historically the federally threatened western prairie fringed orchid (*Platanthera praeclara*; Currier 1982).

Mormon Island is characterized by distinctive and relatively linear landscape features that vary in elevation, often described as ridge and swale topography (Hurr 1983, O'Brien and Currier 1987, Currier 1989, 1995, Henszey et al. 2004). Hydrologically connected to groundwater and periodically retaining surface water, swales within the landscape have concomitantly been referred to as "sloughs" in the region (Whiles et al. 1999, Vivian et al. 2013). However, these depressional and linear topographical landforms do not directly relate to a particular hydrological or vegetation-based wetland classification (Kantrud et al. 1989, Keddy 2010, Tiner 2016) and may support wet meadow, shallow marsh, or even deep marsh vegetative communities depending on their average annual hydroperiod (Kantrud et al. 1989, Davis et al. 2006, Meyer and Whiles 2008, Tiner 2016). Therefore, when contextualizing research in the CPRV, it is important to note that the term "slough" is occasionally used to describe linear wet meadow features in the regional scientific literature, but the term also can be used to describe topographically similar wetlands with more permanent hydroperiods. Barney series soils composed of deep, poorly drained loams on highly permeable alluvial deposits of sand and gravel predominate in Mormon Island's wet meadows (USDA-NRCS 2004). Dominant graminoids in Mormon Island's wet meadows include wooly sedge (*C. pellita*), common threesquare (*Schoenoplectus pungens*), and prairie cordgrass (*Spartina pectinata*). Common forbs (dicots) include common sneezeweed

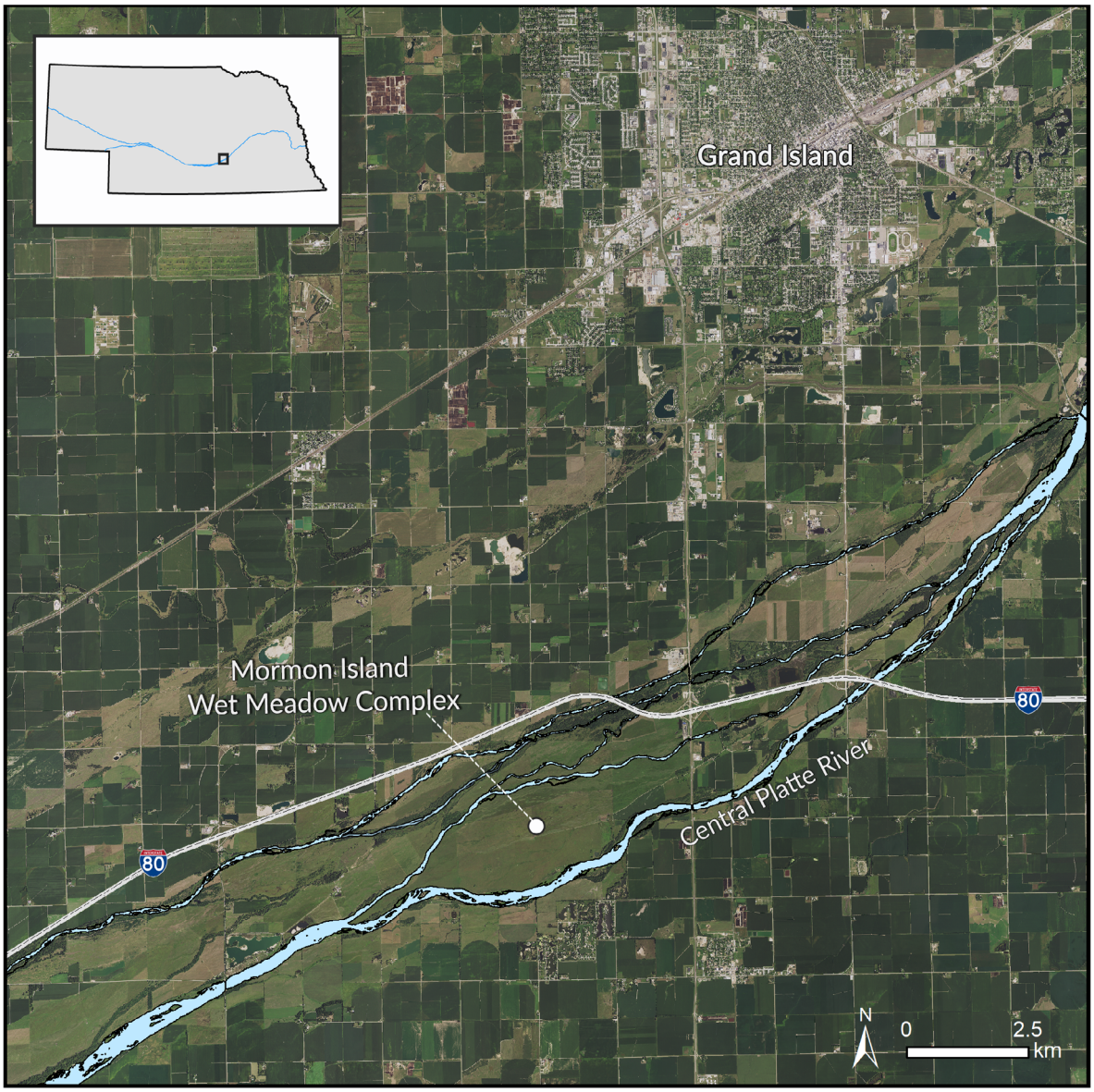

Fig. 1. Aerial view of Mormon Island wet meadow complex located along the Platte River south of Grand Island, Nebraska, USA (40.799, −98.416). Inset (top left) shows study location along the Central Platte River within the state of Nebraska. Landsat-7 image courtesy of the U.S. Geological Survey.

(*Helenium autumnala*), prairie ironweed (*Vernonia fasciculate*), and lanceleaf frog fruit (*Phyla lanceolata*) (Nagel and Kolstad 1987).

Hydrologic variables

Surface weather data were obtained from the High Plains Regional Climate Center. Daily totals of precipitation (rainfall) and snowfall were from the Grand Island Central Nebraska Regional Airport Weather Station (40.9611, −98.3136; climod.unl.edu), and evapotranspiration was collected near Alda, Nebraska (station ID A253409; 40.53, −98.31). Both stations are less than 20 km from Mormon Island. We obtained daily streamflow records from the US Geological Survey National Water Information System for gage 06770500 at

Grand Island, Nebraska, approximately 17.7 km (11 mi) downstream from the camera and well location. Groundwater data were monitored approximately 608 m south from the middle channel of the river and approximately 1038 m north from the south channel of the Platte at an elevation of 576.13 m above mean sea level (m asl; 40.80191, −98.40873). The well was instrumented to measure groundwater levels to an elevation of 575.12 m asl (approximately 1 m below surface) using a Levelogger pressure transducer (Solinst LT Edge Model 3001 M10, Ontario, California, USA). Groundwater measurements were compensated for changes in atmospheric pressure using a barologger (Solinst Barologger Edge Model 3001, California, USA) installed approximately 4.5 km west of the well site.

We monitored water inundation using a digital time-lapse camera at one location within a wet meadow swale in the center of Mormon Island. The camera was located 100 m east of the groundwater well within the same swale formation. The study site was rarely connected to riverine surface water, as circuitous connections between the majority of wetland habitats on Mormon Island and the middle channel of the Platte River occur only during substantial and sustained peak flow events (>425 m^3/s or >15,000 ft^3/s; June 2015) as a result of overbank flooding. The camera was installed as part of the Platte Basin Timelapse project, a multimedia endeavor cataloging a watershed (plattebasintimelapse.com; for camera configurations, see supplemental information). The camera took one photograph every hour of daylight. The immediate frame of view was approximately 26,300 m^2 (2.6 ha) of wet meadow habitat, with an average elevation of 576.88 m asl, slightly above the south channel's mean bed elevation (576.77 m asl) but below the middle channel's mean bed elevation (577.63 m asl) perpendicular to our study site. The resulting image data set consisted of three photos a day, taken between the hours of 10:00 and 14:00 to standardize for shadows and sun position from 17 March 2011 to 3 May 2017. Images with inconsistencies within the frame of view (e.g., rain on the lens, cows in view) were replaced by the next sequential image to complete a set of three per day.

Images were classified using an original macro script and automated batch image analysis in the Java-based open-access program Fiji (Schindelin et al. 2012). A region of interest (ROI) within the image was selected that was comprised of a wet meadow swale that excluded all sky, horizon, and additional landscape to reduce variability (Fig. 2). The colorspace of the ROI was then transformed from red–green–blue (RGB) to hue–saturation–value (HSV) to overcome potential limitations for classifying water (Pekel et al. 2014). Classification consisted of converting the ROI to binary (water, not water) using automated thresholding, calculated as threshold = (average background + average objects)/2. We manually traced visible inundation for periods of dense vegetation growth that obstructed the image frame of view. Tracing was conducted through inference of visible areas and referencing of sequential images. The manually traced masks of water inundation were then measured in ImageJ. An inundation value was calculated as the percent area classified as water within the ROI. Resulting masks of inundated area were visually inspected and manually compared to the original image for accuracy. If a mask was deemed inaccurate, the original image was classified using heads-up digitizing by manually tracing water inundation. We conducted an accuracy assessment using a random number generator to draw five random numbers from 1 to 365, corresponding to days of year (30 January, 7 February, 4 March, 11 April, and 17 May) for a total of 30 images. If an image was unavailable or obstructed (i.e., snow), the closest alternative date was selected. The images were then heads-up digitized by manually tracing visible water inundation with the ROI and measured in ImageJ. Regression analysis was used to compare the results of the heads-up classification with the automated batch classification method.

Analysis

To characterize the wet meadow hydroregime, we calculated a number of metrics to describe the hydroperiod, timing, and frequency of ponding and drying. These metrics were calculated on wet meadow inundation data from 11 March 2011 to 3 May 2017. All other statistical analyses were conducted on a truncated data set, from 11 November 2011 to 3 May 2017, as the groundwater well was not instrumented until eight months after the time-lapse camera. We used a series of

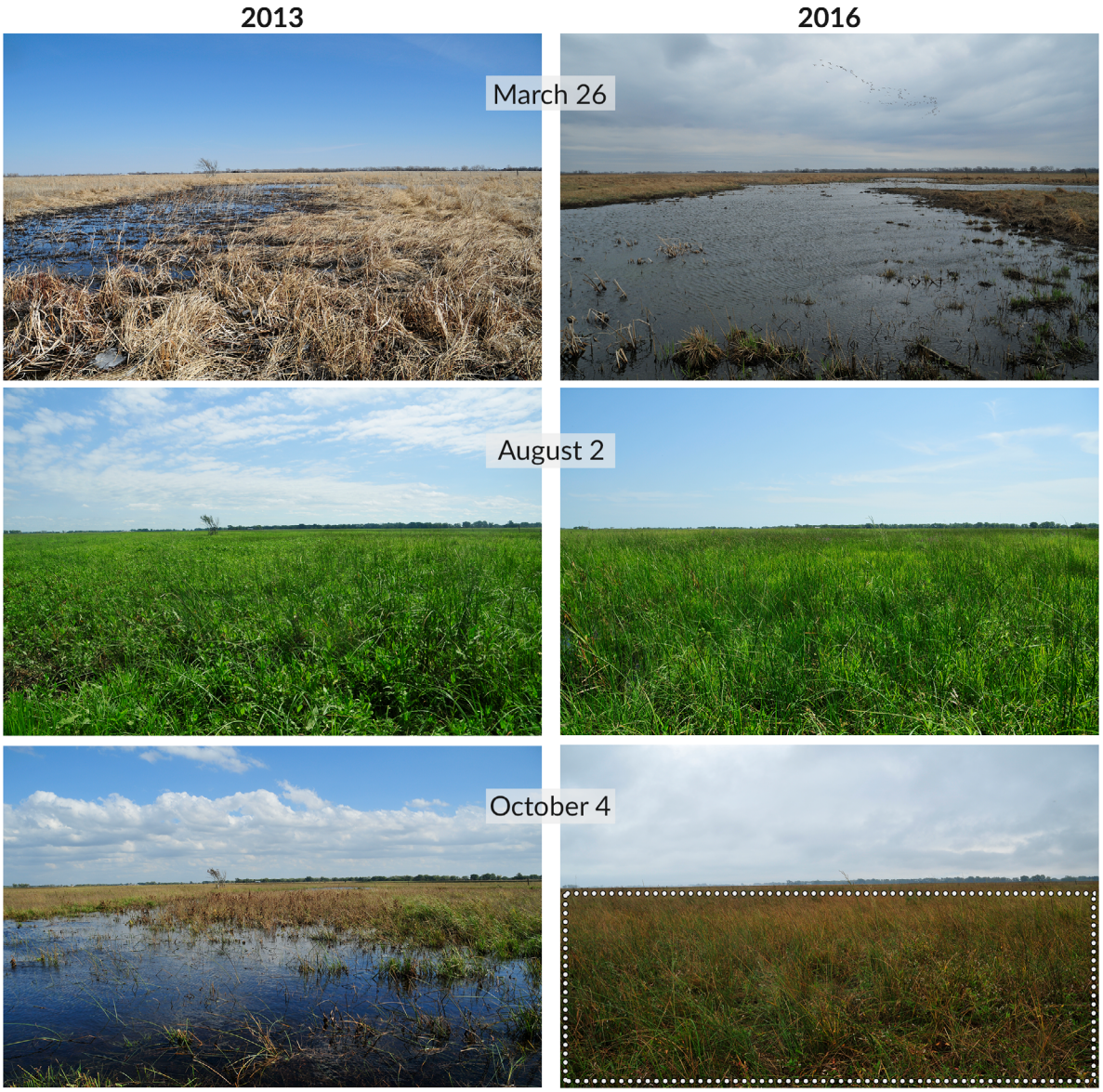

Fig. 2. Time-lapse images showing water inundation at Mormon Island wet meadow in 2013 (left) and 2016 (right) for three dates. The region of interest (ROI) used for image analysis is shown in the bottom right image. Images copyright Michael Forsberg/Platte Basin Time lapse.

statistical approaches to further characterize the wet meadow hydroregime and understand associations between inundation and hydrologic variables, including streamflow, precipitation, groundwater, snowfall, and evapotranspiration. All analyses were conducted using R 3.5.0 (R Core Team 2018), and for days with missing images, inundation data were imputed using the R package imputeTS (Moritz 2016).

To evaluate how hydrologic variables related to inundation, we designated thresholds of wet meadow inundation and calculated the mean of hydrologic variables at these levels. Thresholds of water inundation (WI) were calculated as quartile 1 (Q1; WI = 0%), quartile 2 (Q2; WI > 3.62%), quartile 3 (Q3; WI > 16.6%), and when inundation was greater than the 99th percentile (99th, WI > 39%). The mean value for streamflow,

groundwater, and precipitation were calculated for each of the four thresholds.

Continuous wavelet transform (CWT) was used to identify periodicities in wet meadow inundation, as well as hydrologic variables, and to visualize change over time. CWT detects signals in time-series data relating to ecological processes (Cazelles et al. 2008) and handles non-stationarity and transient properties often present in hydrologic data, while evaluating signals in both the time and frequency domains (Torrence and Compo 1998, Grinsted et al. 2004). The analysis was conducted using the Morlet wavelet in the biwavelet R package (Grinsted et al. 2004). Within the wavelet spectra, areas of statistical significance ($P < 0.05$) were delineated by a black contour outline, and wavelet power, the energy of the signal as a function of time and frequency, was indicated by color, ranging from areas of high power illustrated in red to low power in blue. Areas within the visualized spectrum less reliable to interpretation due to edge effect, an artifact of using CWT, were delineated by a white line and faded color. To assess how hydrologic variables co-varied in frequency and over time, we used wavelet coherence, a measure similar to correlation coefficients (Grinsted et al. 2004). Arrow directionality indicated the phase relationship of the two series; right-facing arrows were "in-phase", meaning that the time-series values varied together, left-facing were "out-of-phase", suggesting they were inversely related, down-facing arrows indicated Y lags X at 90°, and up-facing arrows indicated X lags Y at 90°.

To account for seasonal variability in hydrologic processes and interactions, as well as to understand associations of wet meadow inundation with hydrologic variables at differing times of the year, we delineated six *a priori* seasonal periods defined by climatic averages and regional irrigation schedules (see supplemental information for detailed methods). For each seasonal period (early spring, late spring, summer, early fall, late fall, winter), we calculated summary statistics and identified significant time lags and associations between inundation and hydrologic variables using cross-correlation.

To examine the importance of and predict how wet meadow inundation responded to hydrologic factors during these seasonal time periods, we used Random Forest (RF) regression, a machine-learning algorithm based on an ensemble of decision trees. RF is increasingly used to analyze complex data sets, as it is non-parametric, includes a built-in generalization error (out-of-bag error rate; OOB), and uses two methods of randomization to increase predictive accuracy and overcome over-fitting (Breiman 2001, Cutler et al. 2012). We used the randomForestSRC package in R (Ishwaran and Kogalur 2018), generating 1000 trees, with three variables at each split, and a minimum node size of five. We included year, day of year, streamflow, groundwater, precipitation, snowfall, and evapotranspiration in each seasonally specific model and assessed the contribution of each variable to the models using permutation-based metrics of variable importance (VIMP). VIMP scores rank covariates in terms of the mean decrease in accuracy observed when a particular variable was absent from models, where variables of top importance have higher scores and negative values decrease model accuracy. Partial dependence plots were constructed for the three hydrological variables with the highest VIMP scores using the ggRandomForests package to observe the predicted effect of a variable on water inundation given all other variables are held at their mean (Ehrlinger 2015).

Results

We analyzed 6723 images from 17 March 2011 to 3 May 2017 to assess water inundation. Image analysis resulted in 91% retainment of images using batch-automated classification; 207 resulting masks were identified as inaccurate and corrected where applicable. Inaccuracy was most often due to snow accumulation in the winter or high vegetation growth in the summer, particularly in 2015 when extensive flooding occurred at near peak vegetation height. The accuracy assessment evaluating automated batch classification compared to heads-up classification resulted in an R^2 of 0.97 with a mean error of 0.55% and error range of 0 to 4.84%.

Time-lapse images recorded seasonal and cyclical hydrologic change in the wet meadow. For example, images showed limited water inundation in the wet meadow in the dry spring of 2013 (Fig. 2) and cattle wading in open water during the wet summer of 2015. Broadly,

inundation began in late fall (~November), generally exhibited an annual bimodal peak in early and then late spring, before drying in early summer (Fig. 3). The CPRV experienced periods of extreme drought as well as wetter than average periods during our study. From Summer 2012 to Summer 2013, Hall County, Nebraska experienced extreme to exceptional drought, and contrastingly, 2015 and 2016 were generally high-water years (USGS Stream gage 06770500; US Drought Monitor, https://www.drought.gov/drought/ <accessed March 2018>). Flood events (Platte River gage height >2 m) occurred in late September of 2013, February, May, and June of 2015, and January of 2016.

Hydroregime metrics

The high temporal frequency of the time-lapse images allowed us to characterize the wet meadow hydroregime (Figs. 3a, 4, and Appendix S1: Fig. S1). Hydroperiod had a mean duration of 141 d and varied from 35 d (2013) to 224 d (2015) (Table 1). On average, the wet meadow hydroperiod began on mean day of the year 344 (10 December) and ended on mean day of year 121 (1 May) (Table 1); however, the hydroperiod began as early as 23 October (2016) and as late as 28 February (2013). For wet years (2015–2017), the hydroperiod began earlier, averaging day of the year 309 (5 November), while for dry years (2012, 2013), it began later, averaging day of year 39 (9 February). Within the hydroperiod, water inundation reached a maximum extent on mean day of the year 69 (10 March) (Table 1), with the earliest peak during the study on 24 February (2015) and the latest peak on 29 March (2017). For the duration of the study (2241 d), the wet meadow was dry 45% of the time (1012 d), while 11% of the days showed trace amounts of inundation (238 d, <5% of the ROI classified as water). This varied by year, where in 2011 the wet meadow was dry 75% of the time (217 d of 290 beginning 17 March 2011), and comparatively, it was dry 23% of the time in 2015 (Table 1; Appendix S1: Fig. S1). Groundwater elevation ranged from 575.12 to 576.13 m asl (3.3–0 ft below surface; Table 2). However, from May to December 2012, the groundwater table declined below levels measurable by the pressure transducer (575.12 m asl). Streamflow varied from a minimum of approximately 0 m^3/s to a maximum of 453.0 m^3/s, daily total precipitation from 0 to 83.82 mm, and snowfall from 0 to 254 mm.

Inundation thresholds

Differing thresholds of wet meadow water levels were calculated as Q1 (WI = 0; no ponding water visible), Q2 (WI> 3.62; some water inundation present), Q3 (WI>16.6; high-water inundation), 99th (WI>39; extensive water inundation) (Fig. 5). For Q1, mean groundwater level was 0.60 m belowground surface (1.97 ft or 575.52 masl) and 0.12 m (0.40 ft or 576.0 masl) for the 99th percentile. Mean streamflow was 29.49 m^3/s (1041.33 ft^3/s) for Q1 and 211.48 m^3/s (7468 ft^3/s) for the 99th percentile. Mean precipitation was 1.26 mm for Q1 and 16.93 mm for the 99th percentile.

Wavelet and wavelet coherence

Wavelet transform revealed a statistically significant ($P < 0.05$) annual periodicity of water inundation (λ = ~365 d) from 2014 to 2017 (Fig. 6a), while no annual periodicity was evident in low-water years (2012–2013). Significant periods at λ = 4–32 d occurred during the spring of high-water years (2015–2017), while shorter periods at λ = 4–16 d were significant in 2013 and 2014. Groundwater exhibited significant annual periodicity from 2012 to 2013 and at shorter periodicities (λ = 2–64 d) in the summers of 2013–2016 (Fig. 6b). Streamflow periodicity was significant at λ = 4–64 (d) in 2013–2015 and at λ = 180 d in 2015 and 2016 (Fig. 6c). Significant annual periodicity was evident from 2012 to 2017 for precipitation, evapotranspiration, and snowfall within the wavelet spectra (Fig. 6d–f).

Wavelet coherence analysis between water inundation and hydrologic variables is depicted in Fig. 7. Coherence between water inundation and groundwater varied, but higher power levels were predominately focused in the 2-d to 30-d periodicities (Fig. 7a). Coherent oscillations of groundwater and inundation occurred at similar times of high-water events as streamflow and inundation, with slightly differing frequencies and less power, for example summer 2014 and spring 2016. A coherent annual periodicity was not observed until 2015, where the strength of the in-phase relationship between inundation and groundwater was moderate. Coherence

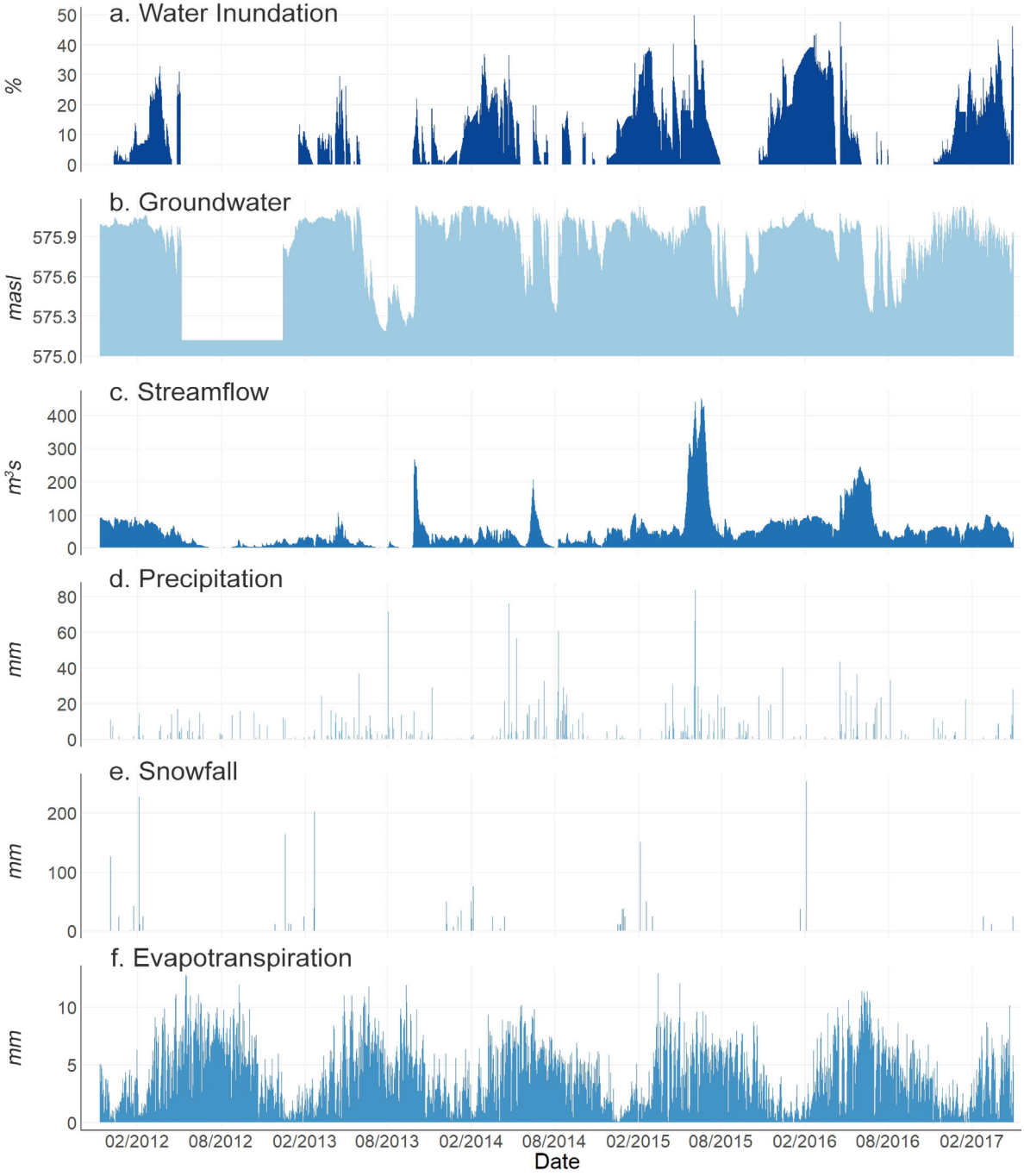

Fig. 3. Hydrologic variables at Mormon Island wet meadow from November 2011 to May 2017. Water inundation in meadow (a) was derived from classification of time-lapse imagery. Groundwater (b) was monitored from a well in the same swale feature at the time-lapse camera. Streamflow (c) was obtained from a USGS streamgage 17.7 km (11 mi) downstream. Precipitation as rainfall (d) and snowfall (e) was obtained from CLIMOD, and evapotranspiration (f) from the High Plains Regional Climate Center.

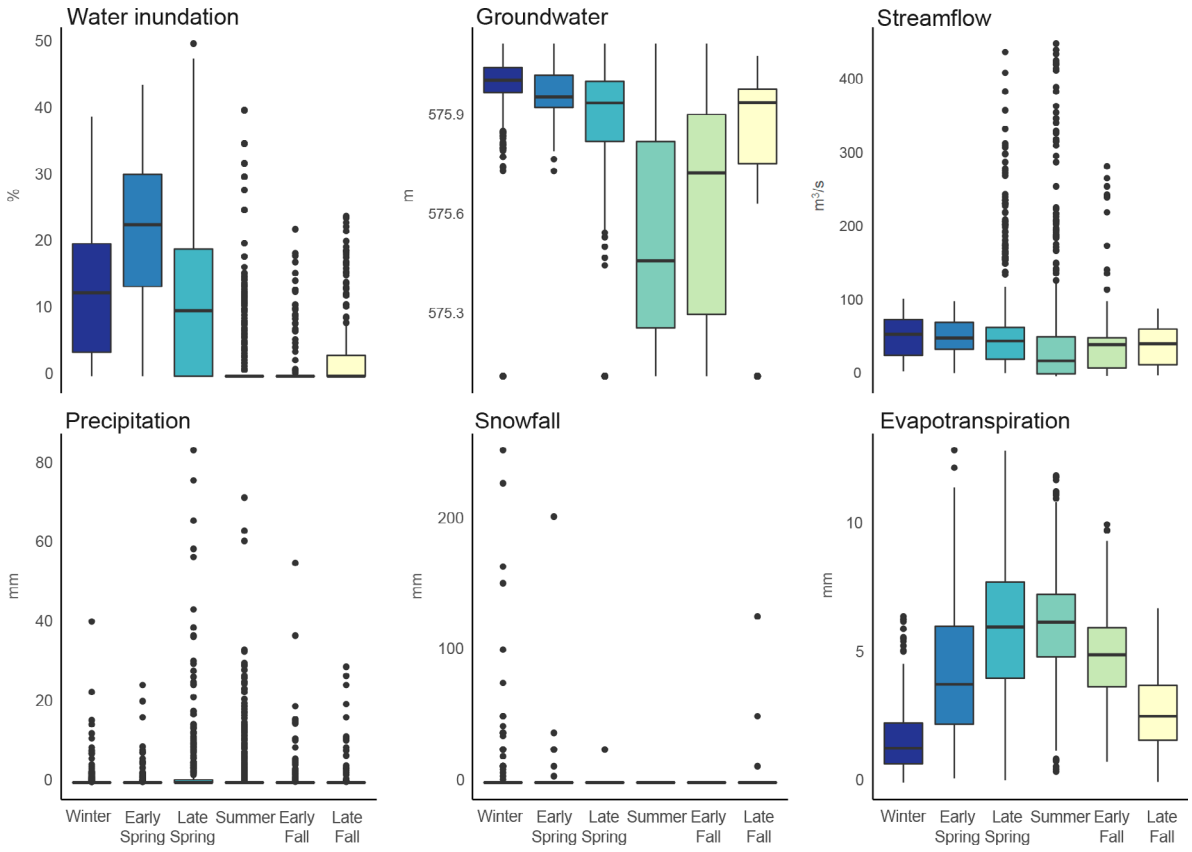

Fig. 4. Boxplot showing the seasonal distribution of water inundation, groundwater elevation, streamflow, precipitation as rainfall, snowfall, and evapotranspiration over six years (2012–2017).

between water inundation and streamflow varied in scale from 1-d to 1-year periods (Fig. 7b). In normal to wet years (2014–2017), inundation and streamflow exhibited coherency at periodicities of one year, where streamflow lagged inundation indicated by arrow directionality. In 2013, streamflow and inundation coherence for periods ranging from 16 to 64 d were in-phase for most of the low-water year. In-phase coherence was evident at 16-d periods during high streamflow events in fall of 2013, summer of 2014, summer of 2015, and spring of 2016. Coherence between water inundation and precipitation (Fig. 7c) was significant at annual periodicities, where water inundation led precipitation. In addition, high-power periods of coherence varied in scale from 1 d to 3 months, with inundation often lagging precipitation. This was evident at periods of 2–16 d from May to August, with exceptions in 2012, which had minimal water, and 2015, which exceeded average, and was observed during this high-water time at coherent periodicities of 16–30 d. Significant coherence at annual periodicities was observed between evapotranspiration and inundation, with fluctuations in evapotranspiration lagging water inundation (Fig. 7d). Inundation and evapotranspiration were often out of phase for periodicities shorter than a year. Overall, inundation and snowfall showed low coherence power, but were significant at annual periodicities where inundation lagged snowfall (Fig. 7e).

Seasonal statistics and correlations

Seasonal variability was evident in all hydrologic variables (Table 2, Figs. 3, 4). Water inundation, on average, was highest in the early spring (mean = 22%), followed by winter (mean = 14%) and late spring (mean = 12%) (Table 2, Fig. 4). Comparatively, groundwater elevation was

Table 1. Characterization of wet meadow hydroregime from 2011 to 2017 identifying key days of the year (DOY) for hydroperiod (HP) and dry period (DP), including 1-start (first day of year of period), z-end (last day of year of period), and ext-duration (the number of days of period).

Characterization	2011	2012	2013	2014	2015	2016	2017
HP_1 (DOY)	–	346	58	3	324	296	309
		12 December	28 February	3 January	20 November	23 October	5 November
HP_z (DOY)	–	107	93	130	183	99	115
		17 April	3 April	10 May	2 July	9 April	25 April
HP_{ext} (days)	–	126	35	127	224	165	171
HP_{max} (DOY)	–	82	72	61	55	56	90
		20 March	12 March	1 March	24 February	25 February	29 March
DP_1 (DOY)	178	126	154	200	211	214	–
	25 June	5 May	3 June	19 July	30 July	2 August	
DP_z (DOY)	345	365	267	229	295	311	–
	11 December	31 December	24 September	17 August	22 October	7 November	
DP_{ext} (days)	167	239	113	29	84	97	–
Dry	0.75	0.69	0.46	0.36	0.23	0.43	–
Wet	0.25	0.31	0.54	0.64	0.77	0.57	–

Notes: Dry is the percentage of days in the year the wet meadow did not have visibly ponding water, while wet is the percentage of days that the wet meadow was inundated. For 2011, the time-lapse camera was not installed until 17 March, when inundation had already begun, and therefore, the hydroperiod was not calculated. Data for 2017 are until May and include the full hydroperiod for this year; however, the data set does not cover the extent of the dry period and therefore this was not included.

Table 2. Range (minimum and maximum values) and mean (with standard error of the mean) of water inundation (WI), groundwater elevation (GW), precipitation as rainfall (Precip), snowfall, streamflow, and evapotranspiration (ET) during six seasonal periods.

Seasonal period	Statistic	WI (%)	GW (m asl)	Precip (mm)	Snowfall (mm)	Streamflow (m^3/s)	ET (mm)
Early spring (N = 269)	Range	0–44	575.74–576.13	0–24.6	0–203.2	4.0–102.2	0.2–13.0
	Mean	22 (±0.7)	575.97 (±0.00)	0.5 (±0.2)	1.3 (±0.8)	55.2 (±1.4)	4.3 (±0.2)
Late spring (N = 334)	Range	0–50	575.12–576.13	0–83.8	0–25.4	4.0–441.7	0.1–12.9
	Mean	12 (±0.6)	575.86 (±0.01)	3.6 (±0.6)	0.2 (±0.1)	74.5 (±4.4)	5.8 (±0.2)
Summer (N = 495)	Range	0–40	575.12–576.13	0–71.9	0	0.0–453.0	0.4–12.0
	Mean	3 (±0.3)	575.54 (±0.01)	2.4 (±0.3)	0	54.1 (±4.0)	6.17 (±0.1)
Early fall (N = 185)	Range	0–22	575.12–576.13	0–55.4	0	0.4–286.0	0.8–10.0
	Mean	2 (±0.3)	575.64 (±0.02)	1.4 (±0.4)	0	44.3 (±3.7)	4.9 (±0.1)
Late fall (N = 260)	Range	0–24	575.12–576.09	0–29.2	0–127.0	1.2–92.0	0.03–6.8
	Mean	3 (±0.3)	575.79 (±0.02)	0.8 (±0.2)	0.7 (±0.5)	42.7 (±1.7)	2.8 (±0.1)
Winter (N = 458)	Range	0–39	575.12–576.13	0–40.6	0–254.0	7.1–105.3	0–6.5
	Mean	14 (±0.5)	575.99 (±0.00)	0.5 (±0.1)	3.6 (±0.9)	53.4 (±1.2)	1.7 (±0.06)
Total (N = 2001)	Range	0–50	575.12–576.13	0–83.8	0–254.0	0–453.0	0–12.9
	Mean	9.2	575.80 (±0.01)	1.6 (±0.1)	1.1 (±0.3)	55.1 (±1.4)	4.3 (±0.06)

highest in winter (mean = 575.99 m asl) followed by early spring (mean = 575.97 m). Platte River streamflow was highest in late spring (mean = 74.5 m^3/s) followed by early spring (mean = 55.2 m^3/s). Precipitation was highest in late spring (mean = 3.6 mm) followed by summer (mean = 2.4 mm), while snowfall was highest in winter (mean = 3.6 mm) and then early spring (mean = 1.3 mm). Correlations among hydrologic variables and wet meadow inundation varied among seasonal phases. Here, we report significant relationships ($P < 0.05$), including time lags, between inundation and streamflow, groundwater, precipitation, and evapotranspiration by seasonal period (Table 3). Of note, for all seasonal periods, no significant associations were

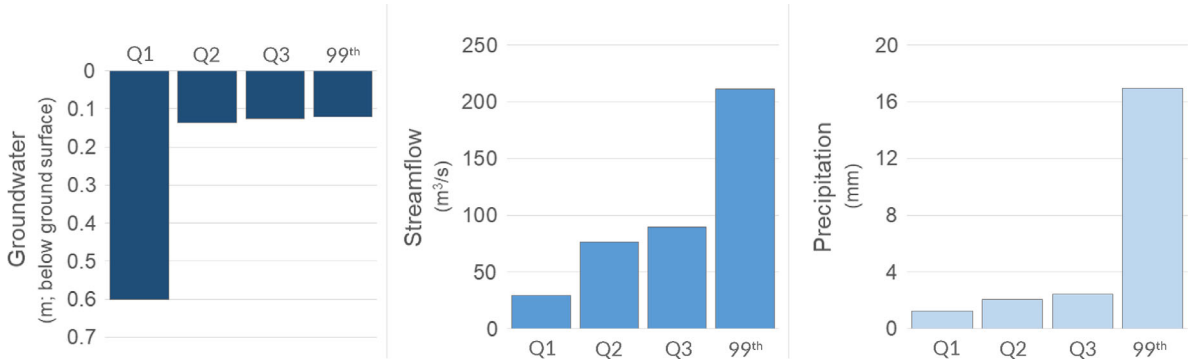

Fig. 5. Mean values of hydrologic variables (groundwater, streamflow, precipitation as rainfall) for water inundation (WI) thresholds. Q1 = quartile 1 (WI = 0), Q2 = quartile 2 (WI > 3.62), Q3 = quartile 3 (WI > 16.6), 99th = values greater than the 99th percentile (WI > 39).

found between snowfall and inundation. In early spring, water inundation was highly correlated with streamflow with a time lag of one day (r = 0.6), that is, one day after Platte River discharge increased the wet meadow inundation increased. During this seasonal phase, inundation was not significantly associated with any other variables (Table 3). In late spring, water inundation was moderately correlated with groundwater (r = 0.46), streamflow (r = 0.33), and precipitation (r = 0.34) and negatively correlated with evapotranspiration (r = −0.39), all with no time lag. In summer, inundation was highly correlated with streamflow (r = 0.79) and groundwater (r = 0.62), as well as to a lesser degree but significantly with precipitation (r = 0.19), again with no time lags (Table 3). In early fall, both streamflow (r = 0.68) and precipitation (r = 0.33) were correlated with inundation at a lag of one day, where streamflow and precipitation preceded water inundation. In addition, inundation was correlated with groundwater with a lag of four days (r = 0.42), where groundwater lagged water inundation. In late fall, inundation was correlated with streamflow (r = 0.43), groundwater (r = 0.33), and precipitation (r = 0.22) and negatively correlated with evapotranspiration (r = −0.21) with no time lags. During the winter, water inundation was moderately correlated with groundwater (r = 0.34), and streamflow lagged water inundation with a delay of one day (r = 0.5). Also of note, during the late fall period groundwater and streamflow showed the highest significant correlation (r = 0.63) (Table 3).

Random forest

RF varied seasonally in their error rate and ability to predict water inundation. A mean of 82.6% variance was explained across all models, and error rates ranged from 3.2 in late fall to 44.1 in late spring (Table 4). The high error rate for late spring is likely attributed to high variability in water inundation, as well as other hydrologic variables, during this period; water inundation, precipitation, and evapotranspiration exhibited the highest range, with the range of streamflow in late spring second highest to summer (Table 4). This was further reflected by the VIMP metrics in late spring, where six parameters were in double-digit significance (Table 4).

For all seasonal periods, streamflow was one of the top two variables of importance (Table 4). Similarly, groundwater was an important variable in all seasons except winter. Year was important for model accuracy in winter, spring, and late fall; however, it was less important in the summer and early fall, indicating water inundation exhibited less annual variability during these seasons.

Partial dependence plots from RF models showed a near-linear relationship between streamflow and water inundation in the winter, early spring, summer, and late fall, and a polynomial response in late spring and early fall (Fig. 8). The seasonal difference in late spring and early fall corresponded to the groundwater exceeding streamflow in measures of variable importance. Although evapotranspiration was not ranked in the top three important variables

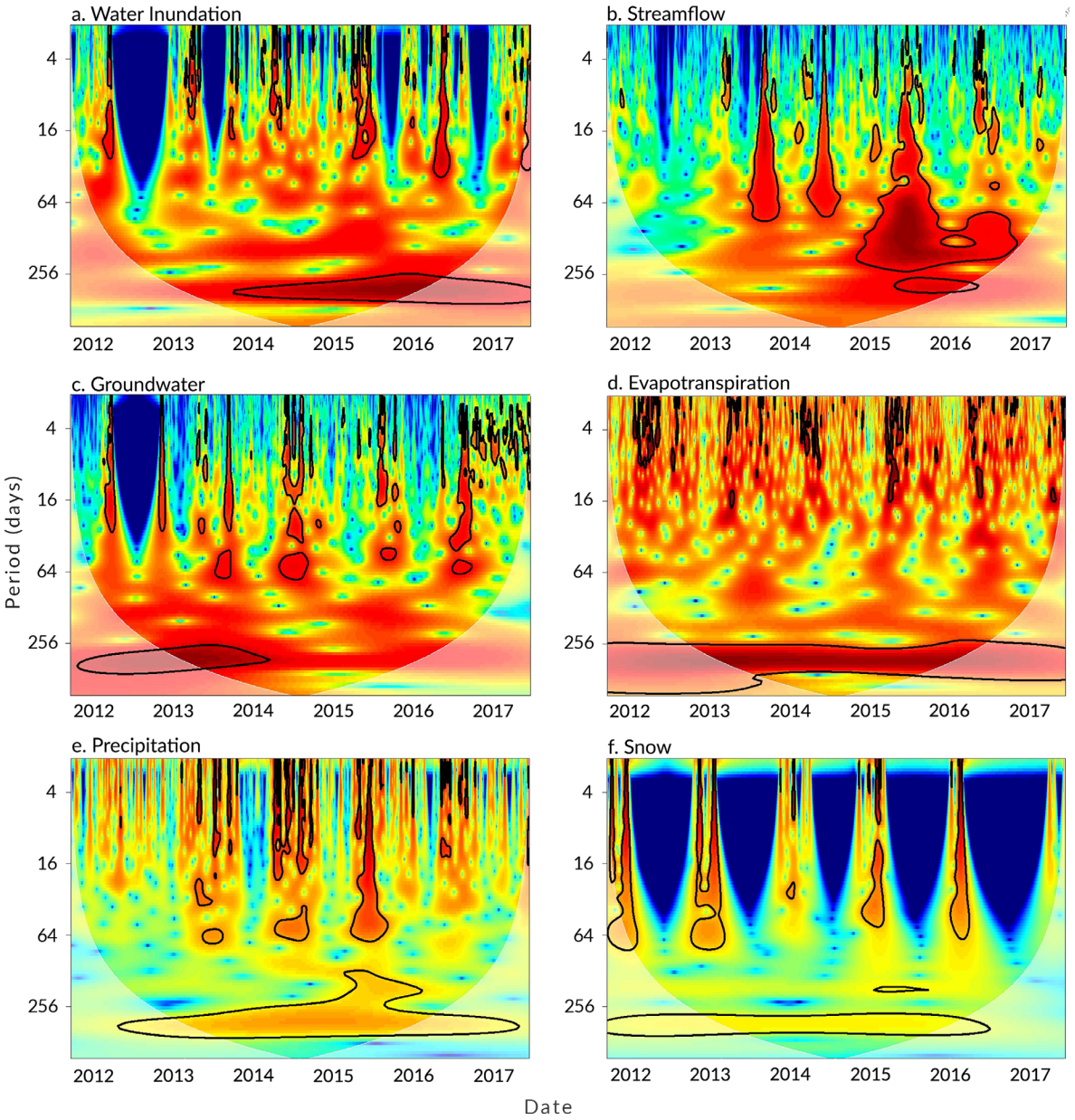

Fig. 6. Wavelet spectrum of water inundation (a), Platte River streamflow (b), groundwater (c), evapotranspiration (d), precipitation as rainfall (e), and snowfall (f) from 2012 to 2017. The black contour line indicates significant ($P < 0.05$) areas, and the gray shaded cone denotes areas influenced by edge effects. Power levels are indicated by color, with areas of high power shown in red and areas with less to no power in blue.

for any seasonal period, during the early and late spring it contributed more to the accuracy of the model, and its inverse relationship was nearly linear, with the strongest effect predicted in late spring (Fig. 8).

The RF model indicated water inundation was not predicted to respond to groundwater until levels are above 575.75 m asl (Fig. 8). This was especially evident in the winter, where groundwater remained relatively high. The influence of

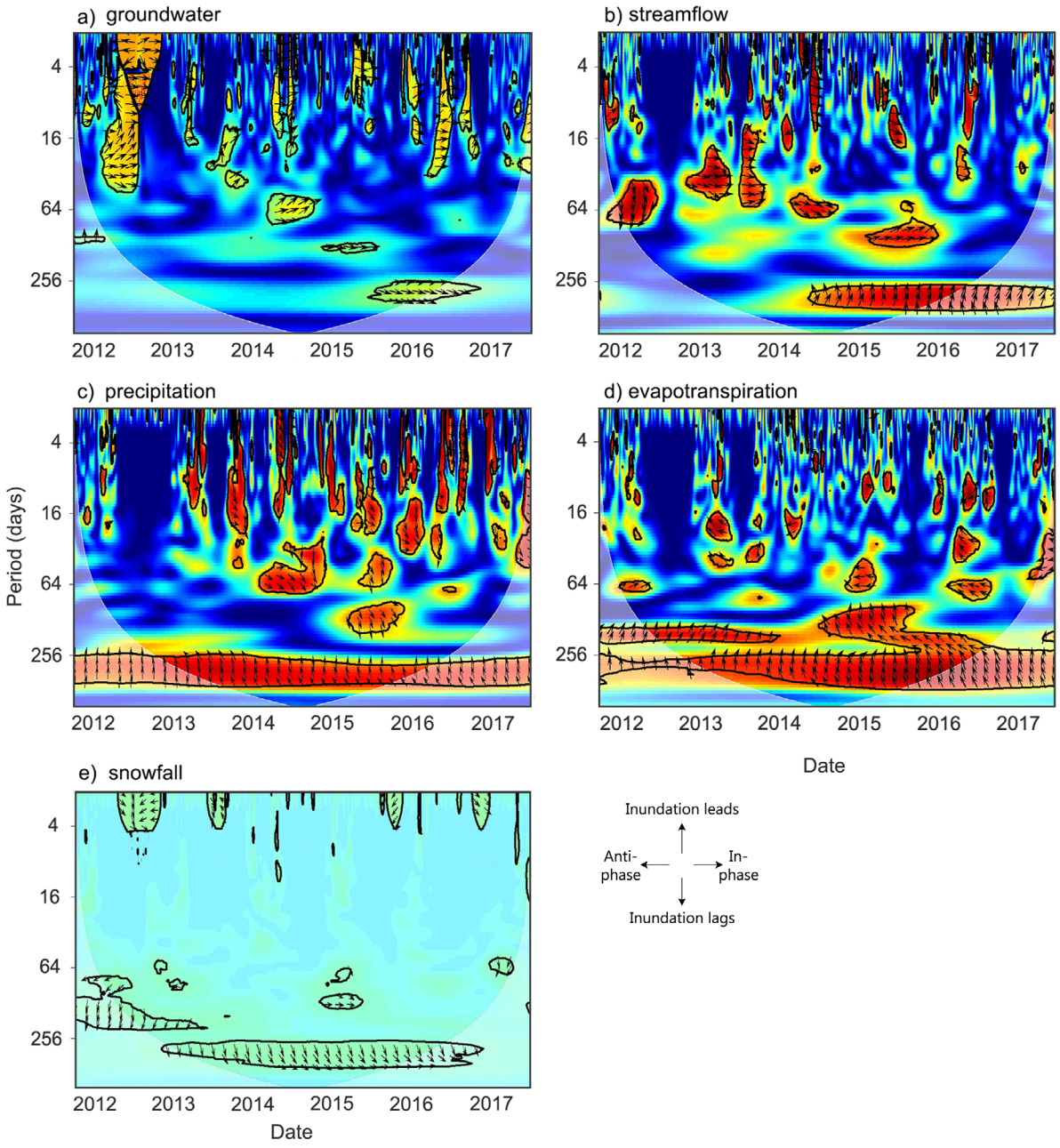

Fig. 7. Wavelet coherence between wet meadow water inundation and hydrologic variables (groundwater [a], streamflow [b], precipitation as rainfall [c], evapotranspiration [d], and snowfall [e]). The black contour line indicates areas of significant ($P < 0.05$) coherence, and the gray shaded cone denotes areas influenced by edge effects. Power levels are indicated by color, with areas of high power shown in red and areas with less to no power in blue. Arrows indicate how the wavelet spectra of water inundation and hydrologic variables relate. Right pointing arrows (in-phase) indicate they are synchronous, left arrows (out of phase) denote an inverse relationship, arrows pointing up indicate the hydrologic variable lags water inundation, and arrows pointing down denote water inundation precedes the hydrologic variable.

Table 3. Cross-correlation analysis with time lags of water inundation and hydrologic variables.

	WI-GW		WI-CMS		WI-PRCP		WI-ET		GW-CMS	
Seasonal period	*r*	*k*	*r*	*k*	*r*	*k*	*r*	*k*	*r*	*k*
Winter	0.34*	0	0.5*	−1	0.08^{NS}	0	-0.05^{NS}	0	0.30*	0
Early spring	-0.09^{NS}	0	0.6*	1	0.0^{NS}	0	-0.11^{NS}	0	−0.3*	−1
Late spring	0.46*	0	0.33*	0	0.34*	0	−0.39*	0	0.33*	0
Summer	0.62*	0	0.79*	0	0.19*	0	-0.07^{NS}	0	0.52*	0
Early fall	0.42*	−4	0.68*	1	0.33*	1	0.13^{NS}	0	0.56*	−4
Late fall	0.33*	0	0.43*	0	0.22*	0	−0.21*	0	0.63*	0

Notes: *r* denotes cross-correlation coefficient; *k* denotes time lag in days, where positive values indicate water inundation lagged hydrologic variables, and negative lags indicate water inundation preceded variables; * denotes significance at $P < 0.05$; NS marks not significant variables; WI, water inundation; GW, groundwater; CMS, streamflow; and PRCP, precipitation as rainfall.

Table 4. Results of random forest regression modeling water inundation over six seasonal periods showing the variable importance scores (VIMP).

Winter		Early spring		Late spring		Summer		Early fall		Late fall	
Variable	VIMP	Variable	VIMP	Variable	VIMP	Variable	VIMP	Variable	VIMP	Variable	VIMP
Year	141.0	Year	108.9	GW	44.0	CMS	35.1	GW	11.2	Year	29.4
CMS	44.4	CMS	52.1	CMS	41.9	GW	33.3	CMS	8.3	CMS	29.3
DOY	30.4	GW	37.2	Year	38.3	DOY	7.6	DOY	2.6	GW	12.0
GW	23.1	DOY	19.6	DOY	32.1	Year	6.3	Year	2.4	DOY	2.3
ET	3.1	ET	9.8	Prcp	12.8	ET	0.3	Prcp	0.0	ET	1.0
SNW	0.0	Prcp	0.4	ET	10.0	Prcp	0.0	SNW	0.0	Prcp	0.4
Prcp	0.0	SNW	0.0	SNW	0.1	SNW	0.0	ET	0.0	SNW	0.0

Notes: The included variables were year, streamflow (CMS), day of year (DOY), groundwater (GW), evapotranspiration (ET), snowfall (SNW), and precipitation as rainfall (PRCP). Explained variance and error rate, respectively, are as follows: winter, 90.6, 12.6; early spring, 86.7, 15.8; late spring, 63.6, 44.1; summer, 90.7, 5.0; early fall, 74.5, 4.5; late fall, 89.1, 3.2.

groundwater on water inundation stabilized at approximately 575.95 m asl, likely due to soils reaching full saturation. Water inundation at a level of 10% was associated with streamflow between 25 and 30 m^3/s in winter, early spring, and late spring (883–1059 ft^3/s; Fig. 8). However, 10% water inundation was associated with much higher streamflow in the summer (~220 m^3/s or 7769 ft^3/s), as well as in the early and late fall periods (both ~110 m^3/s and 3885 ft^3/s; Fig. 8).

Observations of streamflow–groundwater–inundation relationships

Interactions among wet meadow inundation, groundwater, and streamflow are highlighted in the following five events that occurred during our study. In 2013, streamflow increased from 14.52 m^3/s (513 ft^3/s) on 15 January to 31.71 m^3/s (1120 ft^3/s) on 20 January, which raised groundwater by 0.09 m (0.29 ft) and increased water inundation from zero to 14% within three days. On 25 September 2013, four days of high flows peaking at 262.16 m^3/s (9258 ft^3/s) raised the groundwater table 0.69 m (2.25 ft) with a six-day lag and increased water inundation by 17% following a five to ten-day lag. In 2014, on 15 February, streamflow increased from 25.03 m^3/s (884 ft^3/s) to 64.56 m^3/s (2279 ft^3/s), which increased inundation in the wet meadow by 20% within two days. Groundwater was and remained fully saturated for approximately seven days subsequent to increased streamflow. On 13 January 2015, streamflow increased from 24.95 m^3/s (881 ft^3/s) to 105.34 m^3/s (3720 ft^3/s), increasing groundwater by 0.25 m (0.82 ft). Water inundation increased from 15% on 19 January to 34% on 24 January, responding to streamflow at a lag of six days. Finally, following 4.37 cm (1.72 in) of precipitation on 17 April 2016, we observed a 107.6 m^3/s (3800 ft^3/s) increase in streamflow, a 0.33 m (1.08 ft) rise in groundwater, and 47% increase in water inundation within one day.

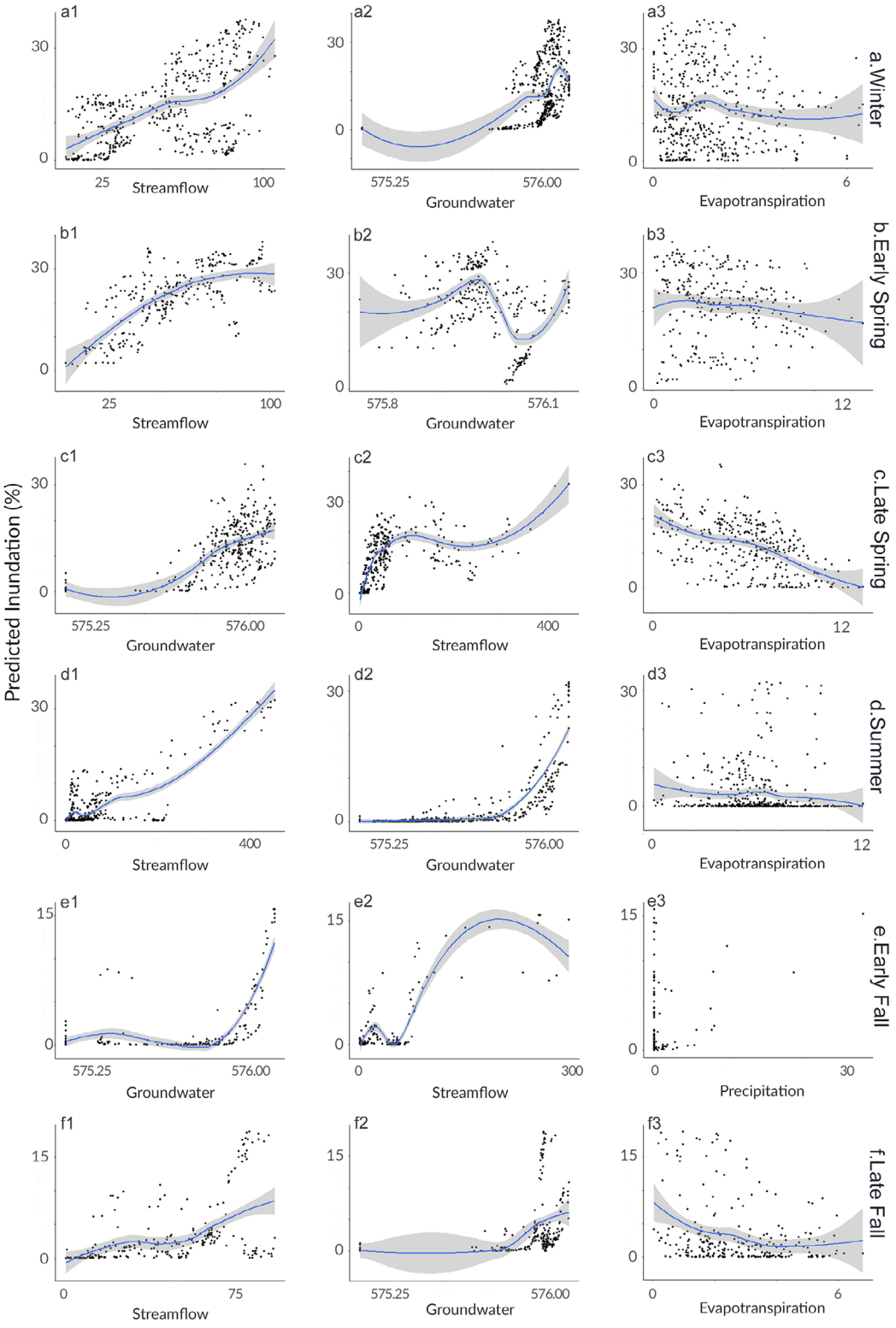

Fig. 8. Partial dependence plots from random forest models illustrating the predicted effect of hydrologic

(Fig. 8. *Continued*)
variables on wet meadow water inundation given all other variables are held at their mean. The plots shown are the three hydrologic variables with the highest variable of importance (VIMP) score for six seasonal periods (winter [a1–3], early spring [b1–3], late spring [c1–3], summer [d1–3], early fall [e1–3], and late fall [f1–3]).

These examples illustrate the dynamic response of wet meadow inundation to interconnected changes in streamflow, precipitation, and groundwater levels at varying times of the year.

Discussion

Hydrologic variability of wetlands facilitates the interaction between aquatic and terrestrial systems, driving ecosystem processes and ecological functions as well as influencing biodiversity (Mitsch and Gosselink 2000). Analysis of time-lapse imagery allowed us to monitor and characterize the hydroregime of an archetypal wet meadow site, a vanishing and increasingly altered habitat type in the CPRV. Our findings revealed high temporal variability and a hydrologically connected riparian ecosystem.

Sustained wet meadow inundation typically began in November, likely as a result of increasing streamflow, rising groundwater levels, stochastic snowfall, and/or less permeable frozen soils typical of that time of year (Fig. 3). However, sustained ponding was delayed by approximately six weeks in dry years (2012 and 2013) as a result of limited increases in these hydrologic drivers. Inundation peaked in early March and again in May, likely in response to precipitation events and a fully saturated water table (Fig. 3). In June, inundation began to rapidly decline with minimal inundation through October; however, stochastic inundation events were present during the summer in response to precipitation. These findings parallel seasonal groundwater patterns observed by Wesche et al. (1994). We found groundwater began to rise generally in late September, earlier than identified by Wesche et al. (1994), and preceded the start of inundation (Fig. 3, 4). Past research indicated that median groundwater levels at Mormon Island ranged from 0.06 to 0.98 m (0.2 to 3.2 ft) belowground from February to April and 0.55 to 1.29 m (1.8 to 4.2 ft) belowground from June to September from 1989 to 1992 (Henszey and Wesche 1993, Wesche et al. 1994, Henszey et al. 2004). Our findings were within the shallower end of this range, with median groundwater elevation at 0.15 m (0.48 ft) below surface for February to April and at 0.63 m (2.08 ft) below surface from June to September. However, it was notable that average Platte discharge was 25.3 m^3/s from 1990 to 1992 during studies by Henszey and Wesche (1993) and Wesche et al. (1994). By contrast, we observed a mean streamflow of 55.1 m^3/s during our study, similar to Chen (2007) who noted average streamflow at 54.3 m^3/s from 1983 to 2003. Although influenced by differences in study time periods, our observations aligned with the findings of Chen (2007) and Henszey and Wesche (1993), indicative of the high connectivity among streamflow, groundwater, and overall hydrologic dynamics, albeit, with limitations in inference given the study was restricted to one site.

Hydrologic signals and correlations at various scales and frequencies indicated inundation was associated with streamflow, and to a lesser extent groundwater, suggesting these may be dominant hydrologic drivers of inundation. In addition, we observed a rapid response of inundation to precipitation events, primarily in the summer. During the study, inundation exhibited greater association with streamflow than groundwater (Fig. 7), with streamflow correlated with inundation at a greater range of frequencies, as well as a consistent annual periodicity starting in 2014 (Fig. 7). Inundation and groundwater exhibited an association during times of hydrologic decline or variability at shorter frequencies (1–16 d; Fig. 7), as well as an association in late spring and summer. This may reflect the lower probability and decreased permanence of inundation in conditions when groundwater is low.

Wet meadow inundation responded to hydrologic drivers with distinctive seasonal regimes. Groundwater was a more important variable in early fall, streamflow in early spring and summer, and both were important drivers in late spring. Evapotranspiration was not an important predictor of wet meadow inundation until late

spring (Fig. 8), which was a similar finding to Henszey and Wesche (1993). The late spring random forest model accounted for the lowest explained variance and highest error rate of all seasonal models, indicating other factors may be influencing inundation during this time period. The significant variations in ambient temperature common to this period could have an impact on biological processes, such as plant growth (Beeson 2006, Hatfield and Prueger 2015), in turn influencing inundation levels (Sánchez-Carrillo et al. 2004). This period likely demonstrates the most complex ecohydrological drivers of inundation, as many environmental attributes, including temperature, plant growth, streamflow, and groundwater, are in flux during this time. During drier late springs, summers, and occasionally early falls, the wet meadow experienced periods of episaturation, as large rain events created temporary spikes in inundation before percolating downward into unsaturated soils (Fig. 7, Tables 3 and 4). For instance, episaturation events that contribute to shallow groundwater replenishment occurred with regularity in the early fall when significant lag times (4 d) were observed between water inundation and subsequent increases in groundwater elevation as groundwater levels were typically low at this time of year as a result of high rates of evapotranspiration and ground water pumping (Table 3, Kranz et al. 2008). Wesche et al. (1994) found that thunderstorms in the summer resulted in peaks in daily groundwater levels, and if no additional precipitation events occurred, the groundwater table returned to previous levels within two weeks. We found water was retained on the landscape an average of nine days after a single precipitation event, but varied seasonally and in relation to groundwater levels. Stochastic precipitation events were coherent with groundwater with high power across 1- to 16-d periods in the summer of 2013, 2014, and 2016 (Fig. 7), but coherence was not observed in years with minimal precipitation (2012; Fig. 3) or summers with high-water levels (2015; Fig. 7). Sustained inundation was likely driven by endosaturation resulting from a complex relationship between streamflow and groundwater throughout the year and was highlighted by the large flows associated with 10% inundation from summer through late fall (Fig. 8).

In addition to seasonally disparate associations, our findings suggest that differing hydrologic drivers may govern the amount as well as duration of water inundation. A lack of inundation within the wet meadow is likely a response to a low groundwater table (Fig. 5). Contrastingly, high-water inundation may be attributed to high streamflow in addition to large precipitation events (Fig. 5). Mean groundwater level varied less than 0.01 m (0.6 in) between Q2, Q3, and 99%. In comparison, the difference in mean streamflow for Q1 and Q2 was 46.9 m^3/s (1656 ft^3/s) and for Q2 and 99^{th} was 182 m^3/s (6426 ft^3/s), demonstrating the importance of high streamflow events that initiate wet meadow inundation. However, groundwater levels above a certain threshold, an estimated 575.75 m asl (~0.48 m belowground surface) in our exemplar system, set the stage for sustained periods of inundation. In this way, groundwater level likely has a significant influence on the temporal duration of inundation but plays a smaller role in moderating the extent of wet meadow inundation.

During the study period, increases in streamflow preceded both water inundation increases as well as groundwater level increases, with the exception of inundation in winter (Table 3). This aligned with the findings of the Platte River Environmental Impact Statement Team Technical Report (Bureau of Reclamation 2001), which found that groundwater rises lag behind river rises unless there is impact from an additional factor such as precipitation. The report suggests 170–283 m^3/s (6000–10,000 ft^3/s) sustained over three days would raise groundwater elevation by approximately 3.81 cm (1.5 in) within 152.4 m (500 ft) from the river. Our results reinforce this finding from a distance of approximately 800 m (2625 ft) from the nearest river channel, discerning a delayed response of inundation and groundwater to changes in streamflow, on average approximately five days for inundation to respond, and a rapid response to precipitation, usually within the day. Furthermore, it may suggest that lag time through the hydrogeological system increases as connectivity via saturated soils decreases. However, the sustained impact would likely differ seasonally and be an aggregated result of groundwater elevation, streamflow amount and duration, and precipitation.

Hydroperiod is a defining characteristic of wetlands, contributing to our understanding and classification of wetland type (Kantrud et al. 1989, Tiner 2016). We found the wet meadow site generally had a shorter hydroperiod (Table 1) than the slough wetland hydroperiods (5–12 months) reported by Whiles and Goldowitz (2005), but demonstrated a similar range (6 months) reported by Meyer and Whiles (2008). We found that water was present in the archetypal wet meadow a mean of 51% of the time and ranged from 25% to 77%, indicative of wetland hydrology bordering between ephemeral and intermittent (Whiles and Goldowitz 2001), and findings suggest that the biological productivity of our study site may vary greatly between dry and wet years. As wet meadows are generally seasonally inundated with more ephemeral hydrology, our results indicate our site may have been on the wetter end of the wet meadow classification continuum (Currier 1989, Kantrud et al. 1989, Euliss et al. 2004, Henszey et al. 2004, Tiner 2016).

The drivers of wet meadow inundation range from relatively singular to highly complex. For instance, wet meadows often exist within an ephemeral zone surrounding a more permanent wetland such as in the Prairie Pothole region of South Dakota, USA (Kantrud et al. 1989). Similarly, wet meadows exist topographically above and generally inland of shallow marshes surrounding the outer edges of the Great Lakes, as they are periodically but less frequently inundated by water level fluctuations (Wilcox et al. 2018). By contrast, wet meadows can represent significant expanses of herbaceous wetland similar to grasslands that are supported by shallow springs linked to perched aquifers in lower elevation arid regions (Lord et al. 2011, Cooper et al. 2012, Caven 2014) and spring glacial melt in high mountain landscapes (Rocchio 2006, Tiner 2016). Inundation at our wet meadow study site resulted from a relatively diverse set of drivers, and the seasonally variable linkages between river discharge, groundwater, and precipitation, and the associated time lags, suggest the ecosystem is relatively distinct and reasonably complex. Despite geographic variation in the drivers of wet meadow inundation, there is considerable overlap regarding functional characteristics reflected by our study site. For instance, many wet meadows in the United States are similarly dominated by *Carex* spp. and sustained by relatively shallow groundwater (generally < 1.0 m depth; Sanderson and Cooper 2008, Lord et al. 2011). Additionally, inundation tends to occur temporarily and seasonally but persist long enough (>2 weeks) for the development of hydric soil features (Rocchio 2006, Schook et al. 2019). As in the CPRV, the regulation of rivers and lakes has resulted in the stabilization and reduction of water levels, promoting the decline of wet meadows globally (Tiner 2016, Wilcox et al. 2018). It is important that water resources are managed to maintain hydrologic variation at a landscape scale to maintain the current extent of wet meadow, a limited yet important habitat for several plant and wildlife species (Jiang et al. 2018, Wilcox et al. 2018, Yang et al. 2020).

Wet meadows have been reduced in the CPRV to 5% of their historic area (Currier et al. 1985, Sidle et al. 1989). A myriad of hydrologic, climatic, and anthropic changes (Johnson et al. 2012, Fassnacht et al. 2018, Pauley et al. 2018, Caven et al. 2019*b*) have resulted in encroachment of woody vegetation and channel incisions that threaten to lower the shallow groundwater table (Williams 1978, Currier 1982, Eschner et al. 1983, Randle and Samad 2003). In turn, this has resulted in the drying of some wet meadow systems, causing a change in stable state to lowland prairie ecosystems, thus rendering the previous wet meadows drier and more viable for agricultural row-crop conversion (Sidle and Faanes 1997). This necessitates the need for baseline data as well as understanding connected hydrologic drivers of remaining wet meadow systems to gauge shifts in conditions, monitor impacts, and restore wet meadow habitat. Our study laid a foundation to apply image-analysis techniques for high-resolution monitoring in addition to providing detailed reference data on a representative wet meadow site. Moreover, the use of time-lapse imagery offered tangible and visual evidence of change that can dually provide a powerful approach for communication and education (see Video S1: time lapse and data graphic of wet meadow inundation). Our results, in tandem with prior research (Henszey and Wesche 1993, Chen 2007), show an interconnected relationship between streamflow, groundwater, and

wet meadow inundation. However, as our study was conducted at one location, we recognize inference is limited, and further investigation, including spatial replicates, would be ideal.

Conclusions

Characterization of the hydroregime of an archetypal wet meadow site in the CPRV of Nebraska through analysis of time-lapse imagery revealed high temporal variability, seasonal patterns, and dynamism of a hydrologically connected system. The hydroperiod of the Mormon Island wet meadow complex averaged 141 d and spanned from 10 December to 1 May, on average. Inundation peaked in early spring (mean 10 March), but demonstrated a bimodal distribution, particularly in wet years, peaking again at variable dates in late spring (~early May). Inundation was strongly related to streamflow throughout all seasons. However, the temporal duration of inundation was influenced significantly by groundwater levels. Our models suggested that water inundation did not respond to groundwater below a threshold of 575.75 m asl, and the influence of groundwater elevation on water inundation stabilized at approximately 575.95 m asl, likely due to soils reaching full saturation. Maintaining wet meadow inundation levels is necessary to promote wetland function and support numerous species, with early spring and late spring of notable ecological importance in the CPRV. Our models predicted 17% inundation, the current seasonal mean and approximate third quartile metric, at Platte River streamflow above 35 m^3/s (1240 ft^3/s) in early spring and 70 m^3/s (~2470 ft^3/s) in late spring, with groundwater levels at seasonal means of 575.97 m asl and 575.86 m asl, respectively. However, Mormon Island is one of the wettest sites in the CPRV and higher flows are likely necessary to promote the same level of inundation at other wet meadows in the CPRV (Wesche et al. 1994). Hydrologic variables demonstrated dynamic temporal relationships at a range of frequencies. Understanding the hydrologic character, variation, and drivers of wet meadow hydroregime is integral to establishing sound water conservation measures that will protect the ecological structure and function of wet meadow systems.

Acknowledgments

This study was funded in part by the University of Nebraska Collaboration Initiative, the University of Nebraska at Kearney, and the Crane Trust. We thank the Crane Trust for maintenance and monitoring of groundwater wells and Michael Forsberg, Michael Farrell, Mariah Lundgren, Jeff Dale, and Platte Basin Timelapse for time-lapse camera systems and image access.

Literature Cited

Armbruster, M. J. 1990. Characterization of habitat used by Whooping Cranes during migration, Volume 90. US Department of the Interior, Fish and Wildlife Services, Fort Collins, Colorado, USA.

Baasch, D. M., P. D. Farrell, A. T. Pearse, D. A. Brandt, A. J. Caven, M. J. Harner, G. D. Wright, and K. L. Metzger. 2019. Diurnal habitat selection of migrating Whooping Crane in the Great Plains. Avian Conservation and Ecology 14:6.

Beeson, R. C. 2006. Relationship of plant growth and actual evapotranspiration to irrigation frequency based on management allowed deficits for container nursery stock. Journal of the American Society for Horticultural Science 131:140–148.

Boswell, J. S., and G. A. Olyphant. 2007. Modeling the hydrologic response of groundwater dominated wetlands to transient boundary conditions: implications for wetland restoration. Journal of Hydrology 332(3–4):467–476.

Breiman, L. 2001. Random forests. Machine Learning 45:5–32.

Brinley Buckley, E. M., C. R. Allen, M. Forsberg, M. Farrell, and A. J. Caven. 2017. Capturing change: the duality of time-lapse imagery to acquire data and depict ecological dynamics. Ecology and Society 22:3.

Brinley Buckley, E. M., B. L. Gottesman, A. J. Caven, M. J. Harner, and B. C. Pijanowski. 2021. Assessing ecological and environmental influences on boreal chorus frog (Pseudacris maculata) spring calling phenology using multimodal passive monitoring technologies. Ecological Indicators 121:107171.

Bureau of Reclamation. 2001. Ground water and river flow analyses. Technical Report of the Platte River EIS Team, Technical Service Center, Denver, Colorado, USA.

Caven, A. J. 2014. Malpais spring vegetation recovery after feral horses: comparing LCTA vegetation data from 1999, 2004, and 2014. Environmental Stewardship Division, White Sands Missile Range, U.S. Army, Las Cruces, New Mexico, USA.

Caven, A. J., et al. 2019*a*. Temporospatial shifts in Sandhill Crane staging in the Central Platte River Valley. Monographs of the Western North American Naturalist 11:33–76.

Caven, A. J., E. M. Brinley Buckley, J. D. Wiese, B. Taddicken, B. Krohn, T. J. Smith, and A. Pierson. 2019*b*. Appeal for a comprehensive assessment of the potential ecological impacts of the proposed Platte Republican Diversion Project. Great Plains Research 29:123–135.

Caven, A. J., B. Ostrom, A. Fowler, J. D. Wiese, and K. C. King. 2019*c*. New Wilson's Phalarope nesting record from the Central Platte River Valley, Mormon Island, Hall County, Nebraska. Nebraska Bird Review 87:100–114.

Cazelles, B., M. Chavez, D. Berteaux, F. Ménard, J. O. Vik, S. Jenouvrier, and N. C. Stenseth. 2008. Wavelet analysis of ecological time series. Oecologia 156:287–304.

Chen, X. 2007. Hydrologic connections of a stream–aquifer-vegetation zone in south-central Platte River valley, Nebraska. Journal of Hydrology 333:554–568.

Cooper, D. J., R. A. Chimner, and D. M. Merritt. 2012. Western mountain wetlands. Pages 313–328 *in* D. P. Batzer, and A. H. Baldwin, editors. Wetland habitats of North America: ecology and conservation concerns. University of California Press, Berkeley, California, USA.

Currier, P. J. 1982. Response of prairie fringed orchid to fire and reduction in grazing (Nebraska). Restoration and Management Notes 2:28.

Currier, P. J. 1989. Plant species composition and groundwater levels in a Platte River wet meadow. Proceedings of the North American Prairie Conference 11:19–24.

Currier, P. J. 1995. Relationships between vegetation, groundwater hydrology, and soils on Platte River wetland meadows. Proceedings of the Platte River Basin Ecosystem Symposium 6:1–23.

Currier, P. J., G. R. Lingle, and J. G. VanDerwalker. 1985. Migratory bird habitat on the Platte and North Platte rivers in Nebraska. Pages 177. Platte River Whooping Crane Critical Habitat Maintenance Trust, Grand Island, Nebraska, USA.

Cutler, A., D. R. Cutler, and J. R. Stevens. 2012. Random forests. Pages 157–175 *in* Ensemble machine learning. Springer, Boston, Massachusetts, USA.

Dahl, T. E. 2000. Status and trends of wetlands in the conterminous United States 1986 to 1997. U.S. Department of the Interior, U.S. Fish and Wildlife Service, Onalaska, Wisconsin, USA.

Davis, C. A., J. E. Austin, and D. A. Buhl. 2006. Factors influencing soil invertebrate communities in riparian grasslands of the central Platte River floodplain. Wetlands 26:438–454.

Ehrlinger, J. 2015. ggRandomForests: visually Exploring a Random Forest for Regression. *arXiv* preprint arXiv:1501.07196.

Eschner, T. R., R. F. Hadley, and K. D. Crowley. 1983. Hydrologic and morphologic changes in channels of the Platte River Basin in Colorado, Wyoming, and Nebraska: a historical perspective. U.S. Geological Survey Professional Paper 1277.

Euliss, N. H., J. W. LaBaugh, L. H. Fredrickson, D. M. Mushet, M. K. Laubhan, G. A. Swanson, T. C. Winter, D. O. Rosenberry, and R. D. Nelson. 2004. The wetland continuum: a conceptual framework for interpreting biological studies. Wetlands 24:448–458.

Faanes, C. A., and M. J. LeValley. 1993. Is the distribution of Sandhill Cranes of the Platte River changing? Great Plains Research 3:297–304.

Fassnacht, S. R., N. B. Venable, D. McGrath, and G. G. Patterson. 2018. Sub-seasonal snowpack trends in the Rocky Mountain National Park Area, Colorado, USA. Water 10:562.

Freeland, J. A., J. L. Richardson, and L. A. Foss. 1999. Soil indicators of agricultural impacts on northern prairie wetlands: Cottonwood Lake Research Area, North Dakota, USA. Wetlands 19:56–64.

Gage, E., and D. J. Cooper. 2013. Historical range of variation assessment for wetland and riparian ecosystems, US Forest Service Rocky Mountain Region. Gen. Tech. Rep. RMRS-GTR-286WWW. Pages 286. US Department of Agriculture, Forest Service, Rocky Mountain Research Station, Fort Collins, Colorado, USA.

Galatowitsch, S. M., D. C. Whited, R. Lehtinen, J. Husveth, and K. Schik. 2000. The vegetation of wet meadows in relation to their land-use. Environmental Monitoring and Assessment 60:121–144.

Geluso, K., and M. J. Harner. 2013. Reexamination of herpetofauna on Mormon Island, Hall County, Nebraska, with notes on natural history. Transactions of the Nebraska Academy of Sciences 33:7–20.

Geluso, K., M. J. Harner, and L. A. Vivian. 2011. Subterranean behavior and other notes for *Ironoquia plattensis* (Trichoptera: Limnephilidae) in Nebraska. Annals of the Entomological Society of America 104:1021–1025.

Gleason, C. J., L. C. Smith, D. C. Finnegan, A. L. LeWinter, L. H. Pitcher, and V. W. Chu. 2015. Technical Note: semi-automated effective width extraction from time-lapse RGB imagery of a remote, braided Greenlandic river. Hydrology and Earth System Sciences 19:2963–2969.

Gray, M. J., L. M. Smith, and R. I. Leyva. 2004. Influence of agricultural landscape structure on a

Southern High Plains, USA, amphibian assemblage. Landscape Ecology 19:719–729.

Greenberg, C. H., S. Goodrick, J. D. Austin, and B. R. Parresol. 2015. Hydroregime prediction models for ephemeral groundwater-driven sinkhole wetlands: a planning tool for climate change and amphibian conservation. Wetlands 35:899–911.

Grinsted, A., J. C. Moore, and S. Jevrejeva. 2004. Application of the cross wavelet transform and wavelet coherence to geophysical time series. Nonlinear Processes in Geophysics 11:561–566.

Hatfield, J. L., and J. H. Prueger. 2015. Temperature extremes: effect on plant growth and development. Weather and Climate Extremes 10:4–10.

Henszey, R. J., K. Pfeiffer, and J. R. Keough. 2004. Linking surface- and ground-water levels to riparian grassland species along the Platte River in Central Nebraska, USA. Wetlands 24:665–687.

Henszey, R. J., and T. A. Wesche. 1993. Hydrologic components influencing the condition of wet meadows along the central Platte River, Nebraska. Report prepared for Nebraska Game & Parks Commission by HabiTech. Inc., Laramie, Wyoming, USA.

Hurr, R. T. 1983. Ground-water hydrology of Mormon Island Crane Meadows wildlife area near Grand Island, Hall County, Nebraska. *In:* Hydrologic and Geomorphic Studies of the Platte River Basin. U.S. Geological Survey, Geological Survey Professional Paper 1277-H, Washington, D.C., USA.

Ishwaran, H., and U. Kogalur. 2018. Package: randomForestSRC - Random Forests for Survival, Regression, and Classification (RF-SRC), Version: 2.6.1. https://CRAN.R-project.org/package=randomForestSRC

Jiang, H., C. He, W. Luo, H. Yang, L. Sheng, H. Bian, and C. Zou. 2018. Hydrological restoration and water resource management of Siberian Crane (*Grus leucogeranus*) stopover wetlands. Water 10:1714.

Johnson, L. A., D. A. Haukos, L. M. Smith, and S. T. McMurry. 2012. Physical loss and modification of Southern Great Plains playas. Journal of Environmental Management 112:275–283.

Joyce, C. B., M. Simpson, and M. Casanova. 2016. Future wet grasslands: ecological implications of climate change. Ecosystem Health and Sustainability 2:e01240.

Kantrud, H. A., G. L. Krapu, and G. A. Swanson. 1989. Prairie basin wetlands of the Dakotas: a community profile. U.S. Fish and Wildlife Service, Biological Report 85, Washington, D.C., USA.

Keddy, P. A. 2010. Wetland ecology: principles and Conservation. Second edition. Pages 497. Cambridge University Press, Cambridge, UK.

Keys, T. A., C. N. Jones, D. T. Scott, and D. Chuquin. 2016. A cost-effective image processing approach for analyzing the ecohydrology of river corridors. Limnology and Oceanography: Methods 14:359–369.

Kindscher, K., A. Fraser, M. E. Jakubauskas, and D. M. Debinski. 1997. Identifying wetland meadows in Grand Teton National Park using remote sensing and average wetland values. Wetlands Ecology and Management 5:265–273.

Kirby, D. R., K. D. Krabbenhoft, K. K. Sedivec, and E. S. DeKeyser. 2002. Wetlands in Northern Plains prairies: benefiting wildlife & livestock. Rangelands Archives 24:22–25.

Kramer, N., and E. Wohl. 2014. Estimating fluvial wood discharge using time-lapse photography with varying sampling intervals. Earth Surface Processes and Landforms 39:844–852.

Kranz, W. L., S. Irmak, S. J. van Donk, C. D. Yonts, and D. L. Martin. 2008. Irrigation Management for Corn. NebGuide. Report No. G1850. Institute for agriculture and natural resources, University of Lincoln-Nebraska Extension, Lincoln, Nebraska, USA. http://extensionpublications.unl.edu/assets/pdf/g1850.pdf

Laubhan, M. K., and L. H. Fredrickson. 1997. Wetlands of the Great Plains: habitat characteristics and vertebrate aggregations. Pages 20–48 *in* Ecology and conservation of Great Plains vertebrates. Springer, New York, New York, USA.

Leduc, P., P. Ashmore, and D. Sjogren. 2018. Technical note: stage and water width measurement of a mountain stream using a simple time-lapse camera. Hydrology and EarthSystem Sciences 22:1–11.

Lingle, G. R., and M. A. Hay. 1982. A checklist of the birds of Mormon Island Crane Meadows. Nebraska Bird Review 50:27–36.

Lord, M. L., D. G. Jewett, J. R. Miller, D. Germanoski, and J. C. Chambers. 2011. Hydrologic processes influencing meadow ecosystems. Pages 44–67 *in* J. C. Chambers, and J. R. Miller editors, Geomorphology, hydrology, and ecology of Great Basin meadow complexes: implications for management and restoration. General Technical Report RMRS-GTR-258. U.S. Department of Agriculture, Forest Service, Rocky Mountain Research, Station Fort Collins, Colorado, USA.

Meine, C. D., and G. W. Archibald. 1996. The cranes: status survey and conservation action plan. International Union for Conservation of Nature (IUCN), Gland, Switzerland.

Meyer, C. K., and M. R. Whiles. 2008. Macroinvertebrate communities in restored and natural Platte River slough wetlands. Journal of the North American Benthological Society 27:626–639.

Meyer, C. K., M. R. Whiles, and S. G. Baer. 2010. Plant community recovery following restoration in temporally variable riparian wetlands. Restoration Ecology 18:52–64.

Mitsch, W. J., and J. G. Gosselink. 2000. The value of wetlands: importance of scale and landscape setting. Ecological Economics 35:25–33.

Moorhead, D. L., D. L. Hall, and M. R. Willig. 1998. Succession of macroinvertebrates in playas of the Southern High Plains, USA. Journal of the North American Benthological Society 17:430–442.

Morisette, J. T., et al. 2009. Tracking the rhythm of the seasons in the face of global change: phenological research in the 21st century. Frontiers in Ecology and the Environment 7:253–260.

Moritz, S. 2016. imputeTS: time series missing value imputation. R package version 1.7. [p1]. http://CRAN.R-project.org/package=imputeTS

Nagel, H. G., and O. A. Kolstad. 1987. Comparison of plant species composition of Mormon Island Crane Meadows and Lillian Annette Rowe Sanctuary in central Nebraska. Transactions of the Nebraska Academy of Sciences 15:37–48.

O'Brien, J. S., and P. J. Currier. 1987. Platte River channel morphology and riparian vegetation changes in the Big Bend Reach and minimum streamflow criteria for channel maintenance. Platte River Whooping Crane Critical Habitat Maintenance Trust, Grand Island, Nebraska, USA.

Parajka, J., P. Haas, R. Kirnbauer, J. Jansa, and G. Blöschl. 2012. Potential of time-lapse photography of snow for hydrological purposes at the small catchment scale. Hydrological Processes 26:3327–3337.

Pauley, N. M., M. J. Harner, E. M. Brinley Buckley, P. R. Burger, and K. Geluso. 2018. Spatial analysis of borrow pits along the Platte River in south-central Nebraska, USA, in 1957 and 2016. Transactions of the Nebraska Academy of Sciences 38:36–46.

Pekel, J. F., C. Vancutsem, L. Bastin, M. Clerici, E. Vanbogaert, E. Bartholomé, and P. Defourny. 2014. A near real-time water surface detection method based on HSV transformation of MODIS multi-spectral time series data. Remote Sensing of Environment 140:704–716.

Pfeiffer, K. 1999. Evaluation of wet meadow restorations in the Platte River Valley. Proceedings of the North American Prairie Conference 16:202–206.

R Core Team. 2018. R: a language and environment for statistical computing. R Foundation for Statistical Computing, Vienna, Austria. https://www.R-project.org/

Randle, T. J., and M. A. Samad. 2003. Platte River flow and sediment transport between North Platte and Grand Island. Nebraska (1895–1999). United State Department of the Interior, Bureau of Reclamation, Technical Service Center, Denver, Colorado, USA.

Riggins, J. J., C. A. Davis, and W. W. Hoback. 2009. Biodiversity of belowground invertebrates as an indicator of wet meadow restoration success (Platte River, Nebraska). Restoration Ecology 17:495–505.

Rocchio, J. 2006. Rocky Mountain alpine-montane wet meadow ecological system: ecological integrity assessment. Dissertation. Colorado State University, Fort Collins, Colorado, USA.

Rolfsmeier, S. B., and G. Steinauer. 2010. Terrestrial ecological systems and natural communities of Nebraska (Version IV). Nebraska Natural Heritage Program, Nebraska Game and Parks Commission, Lincoln, Nebraska, USA.

Sánchez-Carrillo, S., D. G. Angeler, R. Sánchez-Andrés, M. Alvarez-Cobelas, and J. Garatuza-Payán. 2004. Evapotranspiration in semi-arid wetlands: relationships between inundation and the macrophyte-cover: open-water ratio. Advances in Water Resources 27:643–655.

Sanderson, J. S., and D. J. Cooper. 2008. Ground water discharge by evapotranspiration in wetlands of an arid intermountain basin. Journal of Hydrology 351:344–359.

Schindelin, J., et al. 2012. Fiji: an open-source platform for biological-image analysis. Nature Methods 9:676–682.

Schook, D. M., A. K. Borkenhagen, P. A. McDaniel, J. I. Wagner, and D. J. Cooper. 2019. Soils and hydrologic processes drive wet meadow formation and approaches to restoration, Western USA. Wetlands 40:637–653.

Sidle, J. G., and C. A. Faanes. 1997. Platte River ecosystem resources and management, with emphasis on the Big Bend reach in Nebraska. US Fish and Wildlife Service, Grand Island, Nebraska, USA.

Sidle, J. G., E. D. Miller, and P. J. Currier. 1989. Changing habitats in the Platte River Valley of Nebraska. Prairie Naturalist 21:91–104.

Skagen, S. K., and F. L. Knopf. 1993. Toward conservation of midcontinental shorebird migrations. Conservation Biology 7:533–541.

Tiner, R. W. 2016. Wetland indicators: a guide to wetland formation, identification, delineation, classification, and mapping. CRC Press, Boca Raton, Florida, USA.

Torrence, C., and G. P. Compo. 1998. A practical guide to wavelet analysis. Bulletin of the American Meteorological Society 79:61–78.

U.S. Department of Agriculture – Natural Resources Conservation Service. 2004. Barney series. National Cooperative Soil Survey U.S.A. https://soilseries.sc.egov.usda.gov/OSD_Docs/B/BARNEY.html

VanDerwalker, J. G. 1982. The Platte River whooping crane critical habitat maintenance trust. Pages 4–6.

Proceedings of the 1981 Crane Workshop, Tavernier, Florida, USA.

Vivian, L. A., M. Cavallaro, K. Kneeland, E. Lindroth, W. W. Hoback, K. M. Farnsworth-Hoback, R. M. Harms, and J. E. Foster. 2013. Current known range of the Platte River caddisfly, *Ironoquia plattensis*, and genetic variability among populations from three Nebraska rivers. Journal of Insect Conservation 17:885–895.

Vörösmarty, C. J., et al. 2010. Global threats to human water security and river biodiversity. Nature 467:555–561.

Wesche, T. A., Q. D. Skinner, and R. J. Henszey. 1994. Platte River wetland hydrology study: final report. Wyoming Water Resources Center Technical Report. University of Wyoming, Laramie, Wyoming, USA.

Whiles, M. R., and B. S. Goldowitz. 2001. Hydrologic influences on insect emergence production from central Platte River wetlands. Ecological Applications 11:1829–1842.

Whiles, M. R., and B. S. Goldowitz. 2005. Macroinvertebrate communities in central Platte River wetlands: patterns across a hydrologic gradient. Wetlands 25:462–472.

Whiles, M. R., B. S. Goldowitz, and R. E. Charlton. 1999. Life history and production of a semi-terrestrial limnephilid caddisfly in an intermittent Platte River wetland. Journal of the North American Benthological Society 18:533–544.

Wilcox, D. A., K. Buckler, and A. Czayka. 2018. Controlling cattail invasion in sedge/grass meadows. Wetlands 38:337–347.

Williams, G. P. 1978. The Case of the Shrinking Channels: the North Platte and Platte Rivers in Nebraska. Page 48. Circulars of the United States Geological Survey No. 781, Denver, Colorado, USA.

Wright, C. K., and M. C. Wimberly. 2013. Recent land use change in the Western Corn Belt threatens grasslands and wetlands. Proceedings of the National Academy of Sciences 110:4134–4139.

Yang, M., S. Xia, G. Liu, M. Wang, Z. Ding, P. Yu, and X. Tang. 2020. Effect of hydrological variation on vegetation dynamics for wintering waterfowl in China's Poyang Lake wetland. Global Ecology and Conservation 22:e01020.

Young, D. S., J. K. Hart, and K. Martinez. 2015. Image analysis techniques to estimate river discharge using time-lapse cameras in remote locations. Computers & Geosciences 76:1–10.

Zweig, C. L., and W. M. Kitchens. 2009. Multi-state succession in wetlands: a novel use of state and transition models. Ecology 90:1900–1909.

Supporting Information

Additional Supporting Information may be found online at: http://onlinelibrary.wiley.com/doi/10.1002/ecs2.3829/full